

# Search for new physics in dijet and multijet final states using data collected at $\sqrt{s} = 13$ TeV with the ATLAS and CMS detectors

---

**Saptaparna Bhattacharya**<sup>\*†</sup>

*Northwestern University*

*E-mail:* [saptaparna.bhattacharya@northwestern.edu](mailto:saptaparna.bhattacharya@northwestern.edu)

In the Standard Model of Particle Physics (SM),  $2 \rightarrow 2$  processes are described well by Quantum Chromodynamics. Any departure from SM expectations implies the existence of New Physics (NP). We present the search for NP in dijet final states in both high mass and low mass regimes. The use of novel jet substructure techniques to probe very low values of the dijet mass are discussed. The search for new physics in four-jet final states is presented. The search for microscopic black holes in energetic multijet final states is shown. Finally, a search for NP with heavy flavor jets is included. These analyses utilize between 2.3 to 15.7 fb<sup>-1</sup> of data collected at  $\sqrt{s} = 13$  TeV using the ATLAS and the CMS detectors at the Large Hadron Collider at CERN. In the absence of a significant excess of events in data, a wide variety of signal models are excluded. These results represent the most stringent limits on NP scenarios in jet-based final states.

*38th International Conference on High Energy Physics  
3-10 August 2016  
Chicago, USA*

---

<sup>\*</sup>Speaker.

<sup>†</sup>On behalf of the ATLAS and CMS Collaborations

## 1. Introduction

The search for new physics in dijet and multijet final states is of paramount importance at the LHC. The mass reach is expected to be much higher at  $\sqrt{s} = 13$  TeV than at  $\sqrt{s} = 8$  TeV given the rapid rise of the parton luminosity with increasing center-of-mass energy. The analyses presented in this document were carried out using data collected by the ATLAS [1] and CMS [2] detectors, which are the two multi-purpose detectors at the LHC.

## 2. Low-mass dijet searches

The search for low mass dijets is limited by the requirements of the trigger and the data acquisition system that are designed to keep the rate of background events low. One of the ways of circumventing this problem is to require an Initial State Radiation (ISR) jet or photon as shown in the Feynman diagram on the left panel of Fig 1. While the requirement of an ISR object may result in lower signal rates, it is highly efficient at triggering on low-mass dijets than traditional methods would allow. The background is estimated using the following functional form, given by:  $f(z) = c_1(1-z)^{c_2}z^{c_3+c_4 \ln z}$ , where  $z = m_{jj}/\sqrt{s}$  ( $m_{jj}$  is the dijet invariant mass) is fit to the distribution on the right panel of Fig. 1 to obtain the parameters  $c_i$ . The statistical significance of an excess in any specific region of the  $m_{jj}$  spectrum is computed using the BUMPHUNTER algorithm [3, 4].

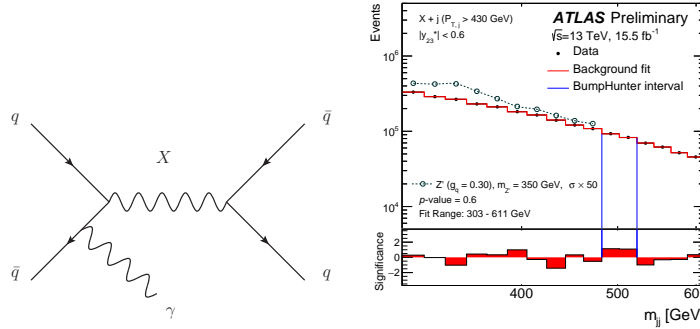


**Figure 1:** Left: The Feynman diagram of the process. Right: The  $m_{jj}$  distribution for events with a photon of transverse momentum ( $p_T$ )  $> 150$  GeV and two jets with  $p_T > 25$  GeV. The vertical lines represent the interval identified by the BUMPHUNTER algorithm to contain the highest discrepancy between the data and the predicted background [5].

An alternate search strategy involves the utilization of the boosted topology, in addition to requiring an ISR jet to suppress trigger rates. The  $Z' \rightarrow q\bar{q}$  system is reconstructed as a single boosted jet and a soft drop criterion is used to identify jets arising from the decay of the  $Z'$ . The background is estimated using data-based control regions with minimal reliance on simulations. The shape of the soft drop mass distribution is shown in Fig. 2. This analysis represents the most sensitive search in the  $m_{jj} < 300$  GeV regime. In the context of models with lepto-phobic  $Z'$ 's, exclusion limits are computed as a function of the coupling to the SM particles where the Lagrangian is of the form:

$$\mathcal{L} = \frac{g_q}{6} \bar{q} \gamma^\mu q Z'_\mu$$

Low mass dijet analyses can also be performed with trigger-level objects that are stored immediately after the High Level Trigger selection. In this data scouting stream, only the 4-momenta of

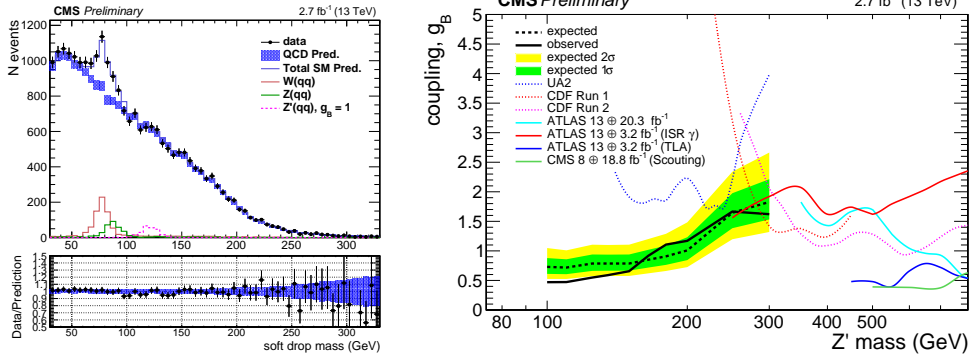


**Figure 2:** The soft drop mass distribution (left) and the exclusion limits yielded by the search (right). The limits obtained from this search dominate the low mass dijet regime [6].

the calorimetric jets is saved in order to sustain the high event rate. The summary of searches performed using this data stream is articulated in Fig. 3. The dijet spectrum is fitted with the following functional form:  $\frac{d\sigma}{dm_{jj}} = \frac{P_0(1-x)^{P_1}}{x^{P_1+P_2}\ln(x)}$ , where  $x = \frac{m_{jj}}{\sqrt{s}}$ , to obtain the background.

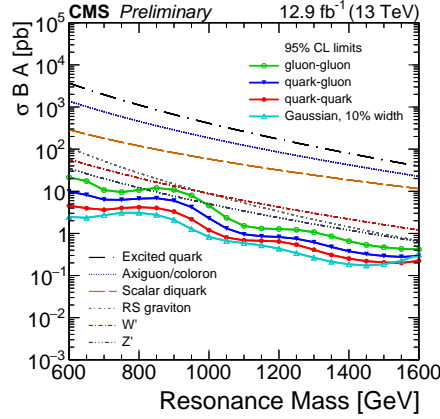


**Figure 3:** The summary of exclusion limits for eight different models of NP computed using the data scouting stream [7].

### 3. High mass dijet searches

The search for high mass dijets is also carried out by looking for an excess of data over a steeply falling dijet background, just as in the low mass case. For the ATLAS result, the following ansatz function is used to parametrize the background:  $f(z) = p_1(1-z)^{p_2}z^{p_3}$  as shown in the left panel of Fig. 4. The CMS search is based on the functional form quoted in Sec. 2. The exclusion limits are set on generic quark-quark, quark-gluon and gluon-gluon resonances and take into account eight different models of NP as shown in the right panel of Fig. 4.

### 4. Four-jet searches

Four-jet signatures arise out of the decay of R-parity violating supersymmetric stop and generic

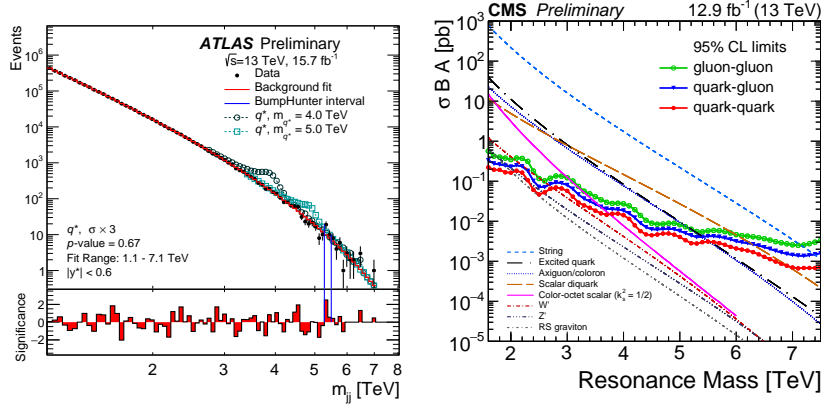


**Figure 4:** Left: The dijet mass spectrum compared to a fitted parametrization of the background in the high mass regime [8]. Right: Summary of the exclusion limits in the high mass dijet regime [7].

colorons. The average mass of a pair of jets is used as the discriminating variable and is shown on the left panel of Fig. 5. The background is computed by using the ABCD method [9, 10], effectively dividing the data into one signal and three background dominated regimes. The analysis excludes stop masses between 250-405 GeV and between 445-510 GeV at a 95% C.L. The mass regime below 250 GeV can be probed by using jet substructure techniques, which allows one to set exclusion limits on squark masses between 80-240 GeV. The average pruned jet mass is shown on the right panel of Fig. 5.

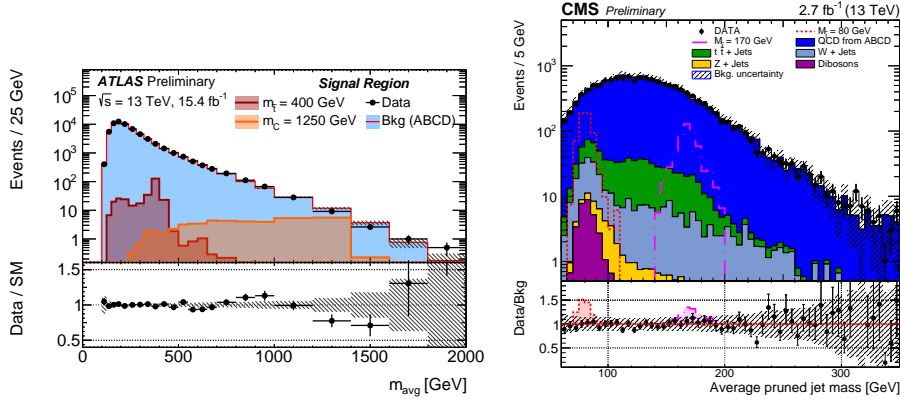


**Figure 5:** Left: The distribution of the average mass computed using a pair of jets [9]. Right: Average jet mass of the two leading pruned jets [10].

## 5. Search for microscopic black holes in multijet final states

In (3+1) dimensional universe, the Planck Scale is much higher with respect to the electro-weak scale. N-flat extra dimensions are introduced in the Arkani-Hamed, Dimopoulos, and Dvali (ADD) model to mitigate this hierarchy problem. The multi-dimensional Planck Scale  $M_D$  is raised according to the following equation:  $M_{pl}^2 = 8\pi M_D^{n+2} r^n$  where,  $M_{pl}$  is the Planck scale observed in (3+1) dimensional space and  $r$  is the compactification radius or the size of the extra dimension. In

models like Randall Sundrum (RS1), this new extra dimension is warped and the true Planck Scale is defined as a function of the warp factor ( $k$ ) and radius ( $R$ ):  $M_D = \frac{M_{pl}}{\sqrt{8\pi}} e^{-\pi k R}$ . Microscopic black holes at energies greater than  $M_D$ , are produced when the impact parameter between two colliding particles is less than the Schwarzschild radius. The Schwarzschild radius of an  $n$ -dimensional black hole is given by:  $R_S = \frac{1}{\sqrt{\pi} M_D} \left[ \frac{M_{BH}}{M_D} \left( \frac{8\Gamma(\frac{n+3}{2})}{n+2} \right) \right]^{\frac{1}{n+1}}$ . Therefore, from semiclassical considerations, the cross section can be calculated as  $\pi R_S^2$ . Semi-classical black holes are short-lived, with a lifetime of  $10^{-27}$  s, and decay via thermal Hawking radiation. They decay equally into all SM degrees of freedom and the final state is comprised of high transverse momenta objects, composed mostly of jets. The variable  $S_T$ , defined as the scalar sum of all objects in an event, is used to distinguish the signal, which would correspond to a broad enhancement in the  $S_T$  spectrum, from the multi-jet background. Since a large number of final state objects is also characteristic of the presence of a semi-classical black hole,  $N$ , defined as the number of objects in an event is used to bin the  $S_T$  spectrum in various multiplicity regimes. The background is estimated using data-driven techniques [11, 12]. In the absence of an excess of events consistent with the existence of a black hole, various model based and model independent exclusion limits are calculated as shown in Fig. 6.

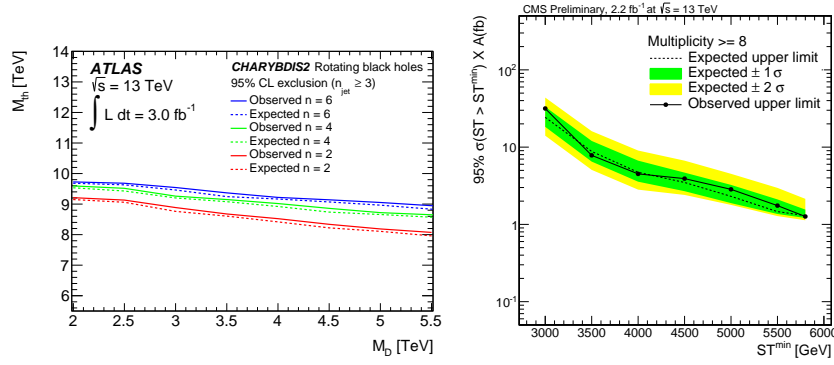


**Figure 6:** Left: The exclusion limits on rotating black holes with varying numbers of extra dimensions ( $n=2, 4,$  and  $6$ ) as a function of the multi-dimensional Planck Scale  $M_D$  and the mass of the black hole  $M_{th}$  [11]. Right: Model independent upper limit on the cross section times acceptance for  $N \geq 8$  scenario [12].

## 6. Searches with heavy flavor jets

The search for NP in dijet final states can also be performed by requiring that one or both of the jets in the final state be  $b$ -tagged, making the analysis sensitive to generic high-mass particles decaying to two jets that originate from one or two  $b$ -quarks. The dijet mass spectra are shown in Fig. 7. These analyses exclude NP resonances between 0.5 to 5.5 TeV.

## 7. Conclusion

The summary of low mass and high mass dijet searches are shown on the left panel in Fig. 8. In the  $m_{jj} < 300$  GeV regime, the analysis carried out with jet substructure techniques dominates as presented in Sec. 2. The exclusion limits obtained for dijets can also be used to exclude models

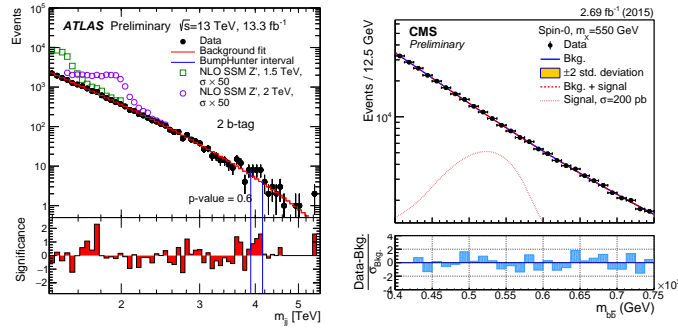


**Figure 7:** Left: The dijet mass spectra overlaid with a background fitted using:  $f(x) = p_1(1-x)^{p_2}x^{p_3}$ , where  $x=m_{jj}/\sqrt{s}$  [13]. Right: The dijet mass spectra where the background is fitted with:  $\frac{x^{p_0+p_1} \ln x}{\int_{x_L}^{x_H} \zeta^{p_0+p_1} \ln \zeta d\zeta}$ , where  $x_L$  and  $x_H$  correspond to the fit ranges [14].

of Dark Matter (DM) by representing limits in terms of exclusion in the mediator versus  $m_{DM}$  plane [15], where  $m_{DM}$  is the mass of the DM particle.

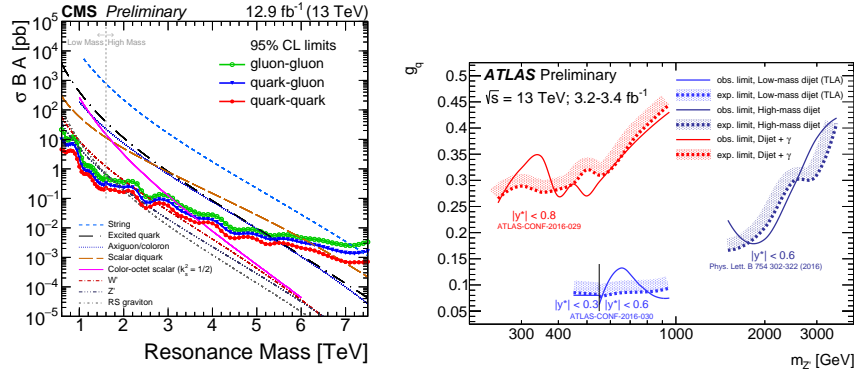


**Figure 8:** Left: Summary of exclusion limits obtained with searches for NP in dijet final states in low mass and high mass regimes [7]. Right: Summary of the exclusion on the coupling of a generic heavy  $Z'$  to the SM.

## References

- [1] ATLAS Collaboration, The ATLAS Experiment at the CERN Large Hadron Collider, JINST 3 (2008) S08003, [10.1088/1748-0221/3/08/S08003](https://doi.org/10.1088/1748-0221/3/08/S08003)
- [2] CMS Collaboration, The CMS experiment at the CERN LHC, JINST 3 (2008) S08004, [10.1088/1748-0221/3/08/S08004](https://doi.org/10.1088/1748-0221/3/08/S08004)
- [3] CDF Collaboration, T. Aaltonen et al., Global search for new physics with 2.0 fb<sup>-1</sup> at CDF, Phys. Rev. D 79 (2009) 011101, [arXiv: 0809.3781](https://arxiv.org/abs/0809.3781)
- [4] G. Choudalakis, On hypothesis testing, trials factor, hypertests and the BumpHunter, 2011, [arXiv: 1101.0390](https://arxiv.org/abs/1101.0390)
- [5] ATLAS Collaboration, Search for new light resonances decaying to jet pairs and produced in association with a photon or a jet in proton-proton collisions at  $\sqrt{s} = 13$  TeV with the ATLAS detector, ATLAS-CONF-2016-070, 2016, <https://cds.cern.ch/record/2206221>

- [6] CMS Collaboration, Search for light vector resonances decaying to quarks at  $\sqrt{s} = 13$  TeV, CMS-PAS-EXO-16-030, 2016, <https://cds.cern.ch/record/2202715>
- [7] CMS Collaboration, Search for narrow resonances decaying to dijets in pp collisions at  $\sqrt{s} = 13$  TeV using  $12.9 \text{ fb}^{-1}$ , CMS-PAS-EXO-16-030, 2016, 2016, <https://cds.cern.ch/record/2205150>
- [8] ATLAS Collaboration, Search for New Phenomena in Dijet Events with the ATLAS Detector at  $\sqrt{s}=13$  TeV with 2015 and 2016 data, ATLAS-CONF-2016-069, 2016, <https://cds.cern.ch/record/2206212>
- [9] ATLAS Collaboration, A search for pair produced resonances in four jets final states in proton-proton collisions at  $\sqrt{s}=13$  TeV with the ATLAS experiment, ATLAS-CONF-2016-084, 2016, <https://cds.cern.ch/record/2206277>
- [10] CMS Collaboration, Search for low-mass pair-produced dijet resonances using jet substructure techniques in proton-proton collisions at a center-of-mass energy of  $\sqrt{s} = 13$  TeV, CMS-PAS-EXO-16-029, 2016, <https://cds.cern.ch/record/2231062>
- [11] ATLAS Collaboration, Search for strong gravity in multijet final states produced in pp collisions at  $\sqrt{s}=13$  TeV using the ATLAS detector at the LHC, 10.1007/JHEP03(2016)026, [http://dx.doi.org/10.1007/JHEP03\(2016\)026](http://dx.doi.org/10.1007/JHEP03(2016)026)
- [12] CMS Collaboration, Search for Black Holes with Early Run 2 Data, CMS-PAS-EXO-15-007, 2015, <https://cds.cern.ch/record/2116453>
- [13] ATLAS Collaboration, Search for resonances in the mass distribution of jet pairs with one or two jets identified as  $b$ -jets with the ATLAS detector with 2015 and 2016 data, ATLAS-CONF-2016-060, 2016, <https://cds.cern.ch/record/2206175>
- [14] CMS Collaboration, Search for a narrow heavy decaying to bottom quark pairs in the 13 TeV data sample, CMS-PAS-HIG-16-025, 2016, <https://cds.cern.ch/record/2204928>
- [15] CMS Collaboration, Dark Matter Summary Plots from CMS for ICHEP 2016, CMS-DP-2016-057, 2016, <https://cds.cern.ch/record/2208044>